1H, 13C and 15N chemical shift backbone resonance NMR assignment of tobacco calmodulin 2

Emmanuelle Boll, Francois-Xavier Cantrelle, Olivier Lamotte, Sébastien Aimé, David Wendehenne, Xavier Trivelli

^{1}H, ^{13}C, and ^{15}N chemical shift backbone resonance NMR assignment of Tobacco Calmodulin 2

Emmanuelle Boll[ab], Francois-Xavier Cantrelle[ab], Olivier Lamotte[c], Sébastien Aimé[c], David Wendehenne[c] & Xavier Trivelli[d**].

[a] CNRS, ERL9002 - Integrative Structural Biology, F-59000 Lille, France.

[b] Univ. Lille, Inserm, CHU Lille, Institut Pasteur Lille, U1167 - RID-AGE - Facteurs de risque et déterminants moléculaires des maladies liées au vieillissement, F-59000 Lille, France.

[c] AgroSup Dijon, CNRS, INRAE, Université de Bourgogne, Univ. Bourgogne Franche-Comté, Agroécologie, 17 rue de Sully, BP 86510, F-21065, Dijon, France

[d] Univ. Lille, CNRS, INRAE, Centrale Lille, Univ. Artois, FR 2638 - IMEC - Institut Michel-Eugène Chevreul, F-59000 Lille, France.

∗∗ To whom correspondence should be addressed.

Key words: Calcium, Calmodulin, CaM, NMR resonance assignment, Tobacco.

Abstract (150-250 words)

Calcium is a ubiquitous second messenger regulating numbers of cellular processes in living organisms. It encodes and transmits information perceived by cells to downstream sensors, including calmodulin (CaM), that initiate cellular responses. In plants, CaM has been involved in the regulation of plant responses to biotic and abiotic environmental cues. Plant CaMs possess a cysteine residue in their first calcium-binding motif EF-hand, which is not conserved in other eucaryotic organisms. In this work, we report the near-complete backbone chemical shift assignment of tobacco CaM2 with calcium. These results will be useful to study the impact of this particular EF-hand domain regarding CaM interaction with partners involved in stress responses. (113 words)

Biological context

Plants are constantly challenged by potentially pathogenic microorganisms. They have evolved complex immune responses that rely on the perception of pathogen attack. One of the earliest cell-signaling event downstream pathogen recognition is a rapid and transient influx of calcium which is decoded by calcium sensors, leading to plant defense activation (Aldon *et al.*, 2018). In plants, calcium sensors include the calcineurin-B-like proteins (CBLs), the calmodulin (CaM) and calmodulin-like proteins (CML), the calcium-dependent protein kinase (CPK) and the calcium and calmodulin-dependent protein kinase (CCaMK) (Ranty *et al.*, 2016)

CaMs are small globular proteins which contain 4 helix-loop-helix domains, the EF-hand domains, each of which binds a single calcium ion (McCormack et al. 2005). Conformational changes upon Ca^{2+} binding enable CaMs to interact with target proteins, the CaM-binding proteins (CaMBPs), mainly by hydrophobic interaction and consequently modulate their activities (Bouché et al. 2005). In plants, Ca^{2+} signals and CaMs have been involved in many physiological processes (Kudla et al. 2018) including plant biotic interactions (Aldon et al. 2018).

Using Mass Spectrometry-based techniques, we have identified *Nt*CaM2 as a putative regulator of plant immune responses triggered in tobacco by cryptogein, a prototypic oomycete virulence factor stimulating tobacco defense responses (Astier et al. 2012). One particularity of plant CaMs is the presence of a Cys residue in the first EF motif whereas it is mostly a Thr in CaMs from other organisms such as animals (Jeandroz *et al.*, 2013) To explore the role of this conserved Cys residue regarding CaM affinity to calcium and CaM interaction with CaMBPs involved in plant immunity, we have initiated NMR studies using *Nicotiana tabacum* Calmodulin2 (*Nt*CaM2) as a model. Here, we present ^{1}H, ^{13}C and ^{15}N assignment and chemical shifts-based predictions of secondary structures of *Nt*CaM2 with calcium.

Methods and experiments

Expression and purification

[^{15}N]- and [^{15}N,^{13}C]-labeled CaM2 were produced using regular molecular biology and biochemistry techniques. *Nt*CaM2 cDNA was amplified by PCR (fw primer catgccatggcagagcagctaacgg; rev primer ggcggatccgcgtcacttggcaagcatcatgcg) and cloned in pET15b. Transformed *E. coli* strain Rosetta bacteria cells were grown in M9 medium at 37°C with [^{15}N]-NH_4Cl (1 g/L), ISOGRO-[^{15}N] powder growth medium (1 g/L) (Sigma-Aldrich) and *U*-[$^{13}C_6$]- (or unlabeled-) glucose (2 g/L) as sole nitrogen and carbon sources. Cell pellet was suspended in sucrose 0.5 M, TRIS-HCl pH 7.5 40 mM, EDTA pH 8 10 mM, PMSF 1 mM and lyzed by sonication. After centrifugation (30,000 g, 30 min, 4°C), supernatant was loaded on a Phenyl Sepharose column (GE Healthcare) equilibrated with buffer C (TRIS-HCl pH 7.5 50 mM, EDTA pH 8 1 mM) and then washed with 5 volumes of buffer C. Flow-through containing *Nt*CaM2 was supplemented with 10 mM of $CaCl_2$ and loaded on a second Phenyl Sepharose column equilibrated with buffer A (TRIS.HCl pH 7.5 50 mM, $CaCl_2$ 1 mM), washed successively with 5 volumes of A, B (A + NaCl 500 mM) and A. *Nt*CaM2 was eluted with buffer C. Fractions containing *Nt*Cam2 were dialyzed (cut-off 8,000 Da) against 500 volumes of dialysis buffer (HEPES pH 7.5 25 mM, EGTA pH 8 2 mM). Sample for NMR measurements consisted of 150 µM of *Nt*Cam2 in HEPES pH 7.4 100 mM, KCl 100 mM, EGTA 10 mM, NTA 10 mM, $CaCl_2$ 7.94 mM ([Ca^{2+}]free = 1.5 mM), 0.001 % TMSP for ^{1}H spectral referencing and 10 % D_2O were added for field locking. $[Ca^{2+}]_{free}$ concentration was calculated according to Dweck *et al.* (2005). All glassware were treated with HCl 0.1 N 20 min, EGTA 0.5 mM 20 min to remove trace of Ca^{2+} and rinsed extensively with milliQ water.

NMR data acquisition and processing

Final volume of 600 µL was placed in 5 mm standard tubes. All NMR spectra were recorded at 293 K using an Avance Neo Bruker 900 MHz spectrometer equipped with CPTCI cryoprobe. The sequence-specific backbone assignment was based on 2D HSQC, and 3D BEST-HNCO, BEST-HN(CA)CO, BEST-HNCACB, BEST-HN(CO)CACB, (H)CBCACONH, pulse-sequences. The chemical shifts were measured relative to TMSP for ^{1}H. Data were transformed and processed using NMRPipe (Delaglio et al. 1995) and qMDD (Qu et al. 2015) for acquisitions with Non-Uniform Sampling (Mavzel et al. 2014) and analyzed using CCPN analysis suite software (Vranken et al. 2005).

Extent of assignments and data deposition

Backbone sequence-specific assignment was completed overall to 97.54 (%) with $^{13}C_{\alpha}$ 98.66 (%), $^{13}C_{\beta}$ 97.86 (%), ^{13}CO 97.99 (%), ^{15}N 95.97 (%) and ^{1}HN 97.96 (%) nuclei. The missing residues amides are located at the very beginning of *Nt*CaM2 (A2, E3) and at the beginning of the first helix (Q9). Figure 1 illustrates the obtained HN-chemical shifts assignments based on multidimensional NMR experiments.

The ensemble of backbone chemical shifts ($^{13}C_{\alpha}$, $^{13}C_{\beta}$, ^{13}CO, ^{15}N and ^{1}HN) of *Nt*CaM2 were used to estimate the secondary structures based on TALOS-N (Shen and Bax 2013) predictions (Figure 2 top). Thus, the analysis showed the presence of eight *alpha*-helices (*alpha*$_1$ 7-20, *alpha*$_2$ 30-39, *alpha*$_3$ 46-55, *alpha*$_4$ 66-76, *alpha*$_5$ 83-93, *alpha*$_6$ 102-113, *alpha*$_7$ 119-129, and *alpha*$_8$ 139-147) and four beta-strands (*beta*$_1$ 27-29, *beta*$_2$ 63-64, *beta*$_3$ 99-101, and *beta*$_4$ 136-138) predicted

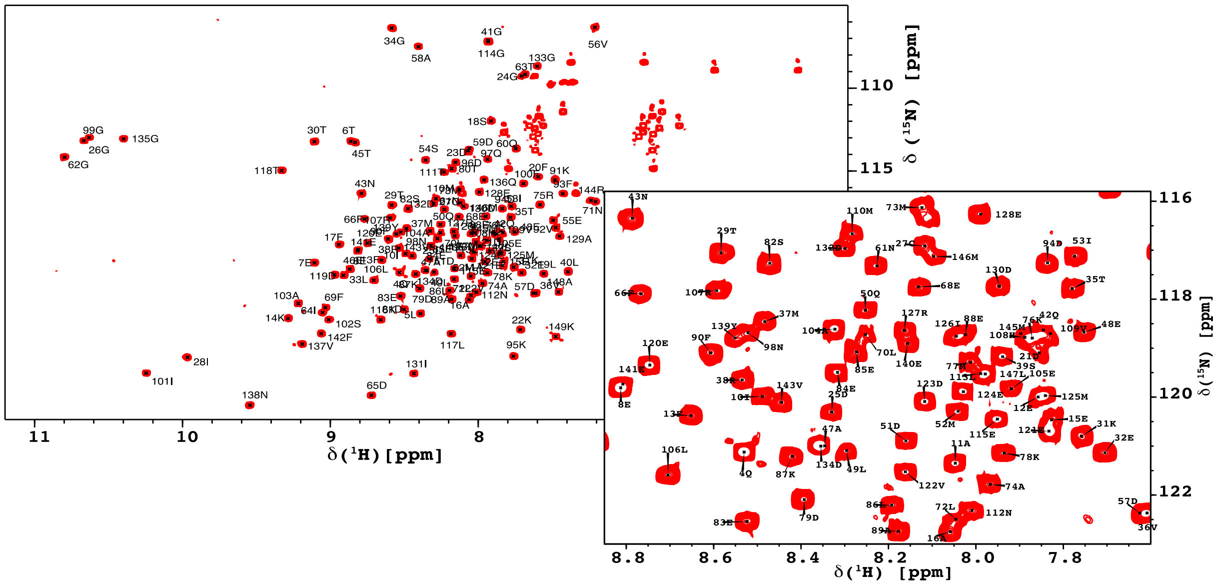

Figure 1. 900 MHz ^{1}H-^{15}N-HSQC spectrum of *Nt*CaM2 at 293 K showing the HN assignment.

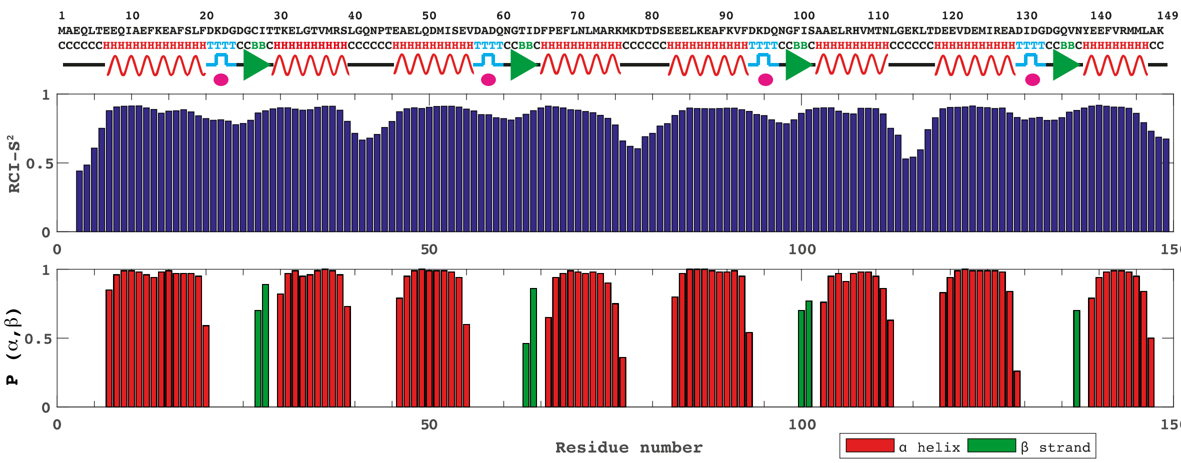

Figure 2. Secondary structure prediction using TALOS-N (Shen and Bax 2013): *alpha*-helices in red, *beta*-strands in green. Pink dots are for the four Ca-binding loops. The middle panel shows predicted random-coil-index-derived order parameters S^2 (RCI-S^2). The bottom panel shows the probability of each residue adopting a secondary structure (P(α,β)).

with high confidence (Figure 2 bottom). The N- and C-termini and the loops between helices 2 and 3, 4 and 5, 6 and 7 are predicted to be flexible (Figure 2 middle). As expected the four Ca-binding loops between helices 1 and 2, 3 and 4, 5 and 6, 7 and 8 appear rigid.

Data availability

A table of the assigned chemical shifts has been deposited into the Biological Magnetic Resonance Database Bank (http://www.bmrb.wisc.edu/) under the BMRB accession number 50750.

References

Aldon D, Mbengue M, Mazars C, Galaud JP (2018) Calcium signaling in plant biotic interactions. Int. J. Mol. Sci. 19: 665. doi: https://doi.org/10.3390/ijms19030665

Astier J, Besson-Bard A, Lamotte O, Bertoldo J, Bourque S, Terenzi H, Wendehenne D (2012) Nitric oxide inhibits the ATPase activity of the chaperone-like AAA+ ATPase CDC48, a target for S-nitrosylation in cryptogein signalling in tobacco cells. Biochem. J. 5: 1346-1358. doi: https://doi.org/10.1042/BJ20120257

Bouché N, Yellin A, Snedden WA, Fromm H (2005) Plant-specific calmodulin-binding proteins. Annu. Rev. Plant Biol. 56:435–66. doi: https://doi.org/10.1146/annurev.arplant.56.032604.144224

Delaglio F, Grzesiek S, Vuister GW, Zhu G, Pfeifer J, Bax A (1995) NMRPipe: a multidimensional spectral processing system based on UNIX pipes. J. Biomol. NMR 6: 277-293. doi https://doi.org/10.1007/BF00197809

Dweck D, Reyes-Alfonso Jr A, Potter JD (2005) Expanding the range of free calcium regulation in biological solutions. Analytical Biochemistry 347: 303-315. doi: https://doi.org/10.1016/j.ab.2005.09.025

Jeandroz S, Lamotte O, Astier J, Rasul S, Trapet P, Besson-Bard A, Bourque S, Nicolas-Francès V, Ma W, Berkowitz GA, Wendehenne D (2013) There's more to the picture than meets the eye: nitric oxide cross talk with Ca2+ signaling. Plant Physiol. 163:459-470. doi: 10.1104/pp.113.220624.

Kudla J, Becker D, Grill E, Hedrich R, Hippler M, Kummer U, Parniske M, Romeis T, Schumacher K (2018) Advances and current challenges in calcium signaling. New Phytologist 218: 414-431. doi: https://doi.org/10.1111/nph.14966

McCormack E, Tsai YC, Braam J (2005) Handling calcium signalling: Arabidopsis CaMs and CMLs. Trends in Plant Sci. 10: 383-389. doi: https://doi.org/10.1016/j.tplants.2005.07.001

Qu X, Mayzel, M, Cai JF, Chen Z, Orekhov VY (2015) Accelerated NMR Spectroscopy with Low-Rank Reconstruction. Angew. Chemie - Int. Ed. 54: 852–854. doi: https://doi.org/10.1002/anie.201409291

Mayzel M, Rosenlöw J, Isaksson L, Orekhov VY (2014) Time-resolved multidimensional NMR with non-uniform sampling. J. Biomol. NMR 58: 129–139 doi: https://doi.org/10.1007/s10858-013-9811-1

Ranty B, Aldon D, Cotelle V, Galaud J-P, Thuleau P and Mazars C (2016) Calcium Sensors as Key Hubs in Plant Responses to Biotic and Abiotic Stresses. *Front. Plant Sci.* 7:327. doi: 10.3389/fpls.2016.00327

Shen Y, Bax A (2013) Protein backbone and sidechain torsion angles predicted from NMR chemical shifts using artificial neural networks. *J. Biomol. NMR* 56: 227–241. doi https://doi.org/10.1007/s10858-013-9741-y

Vranken WF, Boucher W, Stevens TJ, Fogh RH, Pajon A, Llinas M, Ulrich EL, Markley JL, Ionides J, Laue ED (2005) The CCPN data model for NMR spectroscopy: Development of a software pipeline. Proteins: Structure, Function, and Bioinformatics 59: 687–696. doi: https://doi.org/10.1002/prot.20449

Acknowledgments

We acknowledge support for the NMR facilities from IR-RMN THC (CNRS, FR 3050). The authors thank the Chevreul Institute (FR 2638) for its help in the development of this work. Chevreul Institute is supported by the « Ministère de l'Enseignement Supérieur et de la Recherche et de l'Innovation», the « CNRS » the « Région Hauts-de-France », the « Métropole Européenne de Lille » and the « Fonds Européen de Développement des Régions ». The Investissements d'Avenir program, project ISITE-BFC (contract ANR-15-IDEX-0003; grant NOISELESS - RA18041.AEC.IS) is also acknowledge for its support as well as Dr. Claire Rosnoblet for advices.

Conflict of interest

The authors declare that they have no conflict of interest.